J Nanopart Res (2014) 16:2806
DOI 10.1007/s11051-014-2806-3

RESEARCH PAPER

Controlled synthesis of monodisperse gold nanorods with different aspect ratios in the presence of aromatic additives

Yun Wang · Feihu Wang · Yuan Guo · Rongjun Chen · Yuanyuan Shen · Aijie Guo · Jieying Liu · Xiao Zhang · Dejian Zhou · Shengrong Guo

Received: 4 September 2014 / Accepted: 8 December 2014 / Published online: 23 December 2014

Abstract This paper reports the synthesis of monodisperse gold nanorods (GNRs) via a simple seeded growth approach in the presence of different aromatic additives, such as 7-bromo-3-hydroxy-2-naphthoic acid (7-BrHNA), 3-hydroxy-2-naphthoic acid (HNA), 5-bromosalicylic acid (5-BrSA), salicylic acid (SA), or phenol (PhOH). Effects of the aromatic additives and hydrochloric acid (HCl) on the structure and optical properties of the synthesized GNRs were investigated. The longitudinal surface plasmon resonance (LSPR) peak wavelength of the resulting GNRs was found to be dependent on the aromatic additive in the following sequence: 5-BrSA (778 nm) > 7-BrHNA (706 nm) > SA (688 nm) > HNA (676 nm) > PhOH (638 nm) without the addition of HCl, but this was changed to 7-BrHNA (920 nm) > SA (890 nm) > HNA (872 nm) > PhOH (858 nm) > 5-BrSA (816 nm) or 7-BrHNA (1,005 nm) > PhOH (995 nm) > SA (990 nm) > HNA (980 nm) > 5-BrSA (815 nm) with the addition of HCl or HNO_3, respectively. The LSPR peak wavelength was increased with the increasing concentration of 7-BrHNA without HCl addition; however, there was a maximum LSPR peak wavelength when HCl was added. Interestingly, the LSPR peak wavelength was also increased with the amount of HCl added. The results presented here thus established a simple approach to synthesize monodisperse GNRs of different LSPR wavelengths.

Keywords Gold nanorod · Seeded growth · Aromatic additive · LSPR peak wavelength · HCl

Y. Wang · F. Wang · Y. Shen · A. Guo · J. Liu · X. Zhang · S. Guo (✉)
School of Pharmacy, Shanghai Jiao Tong University, 800 Dongchuan Road, Shanghai 200240, People's Republic of China
e-mail: srguo@sjtu.edu.cn; s.guo@leeds.ac.uk

Y. Guo · D. Zhou (✉) · S. Guo
School of Chemistry and Astbury Centre for Structural Molecular Biology, University of Leeds, Leeds LS2 9JT, UK
e-mail: d.zhou@leeds.ac.uk

R. Chen
Department of Chemical Engineering, Imperial College London, South Kensington Campus, 11, London SW7 2AZ, UK
e-mail: rongjun.chen@imperial.ac.uk

Introduction

Gold nanorods (GNRs) exhibit two distinct optical adsorption bands stemming from the longitudinal and transverse surface plasmon resonances (LSPR and TSPR) (Sharma et al. 2009). The maximum LSPR absorption wavelength is linearly related to the aspect ratio (AR: ratio of length to diameter) of the GNRs (Charan et al. 2012; Lohse and Murphy 2013; Menon et al. 2012; Ye et al. 2012). The GNRs, with unique AR-dependent optical properties, have attracted a great deal of interests in many research areas,

including bioprobe (Tian et al. 2012), biomedical imaging (Charan et al. 2012; Wang et al. 2013), spectroscopic detection (Huang et al. 2012), drug delivery (Zhong et al. 2013), gene therapy (Wang et al. 2013; Xu et al. 2013), and photothermal therapy (Liu et al. 2014; Song et al. 2013; Wang et al. 2011).

GNRs are generally synthesized via a seed-mediated growth method (Grzelczak et al. 2008) pioneered by Murphy et al. (2001), improved by Nikoobakht and El-Sayed (2003), and then developed by Ye et al. (2012). Surfactants are commonly used in such a method, and the most widely used surfactant being cetyltrimethylammonium bromide (C16TABr) (Gomez-Grana et al. 2011). It was proposed that GNRs are stabilized by a partially interdigitated bilayer of C16TABr (Gomez-Grana et al. 2011; Johnson et al. 2002; Murphy et al. 2005). The anisotropic growth of the GNRs is due to the preferential adsorption of the cetyltrimethylammonium$^+$ ($C16TA^+$) head group to the {110} face of the seed gold nanoparticle as it has higher surface energies than do other faces (Gai and Harmer 2002; Huang et al. 2009). C16TABr adsorption stabilizes this face, and consequently crystal growth on this face is retarded. As a result, gold atoms are preferentially deposited to the two end facets, leading to rod growth. This mechanism is also supported by density functional theory simulation recently reported by Almora-Barrios et al. (2014).

It has been found that the micellization behavior of C16TABr surfactant can be modified via adding certain aromatic compounds (Yoo et al. 2010). Ye et al. (2012) proved that some aromatic additives can mediate the binding between the C16TABr bilayers and certain facets of growing GNRs. The aromatic ring and carboxyl groups within the additives are the possible binding sites to the surface gold (Michota and Bukowska 2003; Wang et al. 2010). The interaction between halide ions and gold surfaces has also been investigated (Almora-Barrios et al. 2014; Si et al. 2012). Interestingly, bromide anion (Br^-) is hugely influential in the GNR growth. For example, Garg et al. (2010) found that Br ion was a crucial shape-directing agent for GNR formation in the seed-mediated process, irrespective of its origin (C16TABr or NaBr). The size and shape of GNRs could also be modulated by the pH (Edgar et al. 2012; Wang et al. 2005; Ye et al. 2013; Zhu et al. 2010). An increase of OH^- ions of the growth solution could decrease the amount of $C16TA^+$ surfactants adsorbed on the {110} face of the GNR (Wang et al. 2005). Despite significant research over the last 10 years, there have been contradictory reports about how pH may affect the GNR growth (Ye et al. 2013; Ye et al. 2012; Zhu et al. 2010). Moreover, effects of different aromatic additives on the GNR shape and AR are still not fully understood.

Herein, we have systematically studied how GNR growth can be affected by five different aromatic additives with and without the addition of hydrochloric acid (HCl) by the seeded growth method. We show that the pH and aromatic additives are both important in determining the GNR AR and shape. It is possible to synthesize monodisperse GNRs with LSPR spanning from $\sim$ 660 to 960 nm.

Experimental section

Materials

The following chemicals were purchased commercially and used as received unless otherwise stated. Cetyltrimethyl-ammonium bromide (C16TABr, $\geq$ 99 %), 7-bromo-3-hydroxy-2-naphthoic acid (7-BrHNA, $\geq$ 98 %), silver nitrate ($AgNO_3$, 99.9999 %), and ascorbic acid (AA, reagent grade) were purchased from Sigma-Aldrich. 5-bromosalicylic acid (5-BrSA, $>$ 98.0 %) was purchased from TCI Shanghai. 3-hydroxy-2-naphthoic acid (HNA, 98 %) was purchased from J&K Scientific Ltd. Salicylic acid (SA, 99.5 %) and sodium borohydride ($NaBH_4$, 98 %) were purchased from Aladdin. Phenol (PhOH, AR), chloroauric acid tetrahydrate ($HAuCl_4{\cdot}4H_2O$, AR), hydrochloric acid (HCl, 36.0 $\sim$ 38.0 wt % in water), and nitric acid (HNO_3, 65 $\sim$ 68 wt % in water) were purchased from Sinopharm Chemical Reagent Co., Ltd. All solutions were prepared with deionized (DI) water.

Synthesis of GNRs by an improved seeded growth method using aromatic additives

The seed solution for GNR growth was prepared as reported previously (Nikoobakht and El-Sayed 2003). In brief, a 5-mL solution of 0.5 mM $HAuCl_4$ was mixed with 5 mL of 0.2 M C16TABr solution. A 0.6 mL of freshly prepared 0.01 M ice-cold $NaBH_4$ aqueous solution was then injected into the Au^{3+}-C16TABr solution under vigorous stirring (1,200 rpm). After 2 min, the stirring was stopped and the solution's color

changed from yellow to brownish-yellow. The seed solution was aged at 30 °C for 1.5 h before use.

For the preparation of the growth solution, 0.54 g of C16TABr together with a certain amount of each additive was dissolved in 15 mL of warm water (~ 60 °C) in a 50-mL erlenmeyer flask (Ye et al. 2012). The solution was then cooled to 30 °C when a 4 mM $AgNO_3$ solution was added. The mixture was kept undisturbed at 30 °C for 15 min, after which 15 mL of 1 mM $HAuCl_4$ solution and a small amount of HCl (12.1 M) were added. After 15° of slow stirring (400 rpm), 0.064 M AA was added, and then vigorously stirred for 30 s until the solution's color became uniform and stable.

At last, the seed solution was injected into the growth solution. The resultant mixture was stirred for 30 s and then left undisturbed at 30 °C for 12 h for the GNR growth. The resulting GNRs were separated from the reaction solution via centrifugation at 11,500 rpm for 25 min, and washed with DI water twice to remove any residual reactants. The precipitates were re-dispersed in 2 mL of DI water.

Characterization

Ultraviolet–visible–near infrared (UV–Vis–NIR) spectra were recorded on a Hitachi U-2910 UV–Vis–NIR spectrophotometer. The morphology and size of the GNRs were measured using transmission electron microscopy (TEM) (JEM-2100F, JEOL, Japan).

Results and discussion

Effects of aromatic additives

GNRs are mostly prepared via a seeded growth approach using small gold nanoparticle seeds in the presence of C16TABr in aqueous media. The overall chemical reaction (Edgar et al. 2012) for the GNR synthesis can be described in Eq. (1) as follows:

$$2HAuCl_4 + 3C_6H_8O_6 \xrightarrow[Au^0_{(nanosphere)}]{C16TABr\ Ag^+} 2Au^0_{(nanorod)} + 3C_6H_6O_6 + 8HCl, \quad (1)$$

where $C_6H_8O_6$ is AA, a reducing agent that is oxidized to dehydroascorbic acid ($C_6H_6O_6$) after the reaction, and C16TABr is used to direct GNR formation.

In a typical 'seeded' growth process, GNRs are prepared by adding gold nanoparticle seeds to an aqueous 'growth solution' which consists of a mixture of C16TABr, $HAuCl_4$, AA, and silver nitrate (Edgar et al. 2012; Nikoobakht and El-Sayed 2003). A number of factors that affect the GNR synthesis have been investigated. These include temperature, pH, gold nanoparticle seed, reactant concentration, single-component surfactant other than C16TABr, binary surfactant mixtures, etc. (Edgar et al. 2012; Lai et al. 2014; Murphy et al. 2010; Wadams et al. 2013; Wang et al. 2005; Ye et al. 2013; Zhu et al. 2010). More recently, Ye et al. (2012) reported that monodispersity and spectral tenability of GNR could be achieved by using SA or 5-BrSA as additive. It might be because such aromatic additives can be embedded within the C16TABr-capping layers of GNRs, leaving the polar groups pointing away from the hydrocarbon chain of C16TABr (Hassan and Yakhmi 2000; Lin et al. 1994), although the detailed mechanism is still unclear. Herein, we have investigated effects of five different aromatic compounds with different functional groups and aromatic rings on the synthesis of GNRs in an attempt to find out the most effective additives. The chemical structures and structural characteristics of these aromatic additives are shown in Fig. 1 and Table 1. These compounds contain two different aromatic rings (benzene and naphthalene ring) and three different functional groups (–Br, –COOH, and –OH).

Without the addition of HCl, the prepared GNR aqueous solutions are different in color, from red to blue, depending on the types of aromatic additives. Figure 2 shows that the synthesized GNRs are relatively monodisperse, and their UV–Vis–NIR spectra all show two distinct absorption bands, a weaker band peaking at about 525 nm and a stronger band peaking at a longer wavelength. These two bands are attributed to TSPR and LSPR, respectively. A close look of the GNR TEM images reveals that the GNRs prepared in the presence of PhOH, SA, HNA, or 7-BrHNA are stubby sausage- or dog bone-like shaped. Only those prepared in the presence of 5-BrSA have long cylindrical shape rod-like.

The concentrations, pH, dimensions, ARs, and LSPR peak wavelengths of the GNR solutions prepared in the presence of aromatic additives are summarized in Table 2. The AR of the GNRs was measured from the TEM images in Fig. 2a–e. As

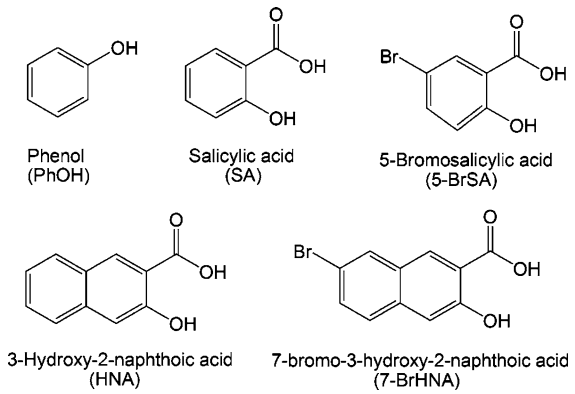

Fig. 1 Chemical structures of the five aromatic additives used in this study

Table 1 The chemical structure characteristics of the five aromatic additives used in this study

Aromatic additive	Aromatic ring	Groups
PhOH	Benzene	–OH
SA	Benzene	–OH, –COOH
5-BrSA	Benzene	–OH, –COOH, –Br
HNA	Naphthalene	–OH, –COOH
7-BrHNA	Naphthalene	–OH, –COOH, –Br

shown in Table 2, the GNR LSPR peak wavelength is found to be dependent on the aromatic additives in the following order: PhOH (638 nm) < SA (688 nm) < 5-BrSA (778 nm); and HNA (676 nm) < 7-BrHNA (706 nm). PhOH, SA, and 5-BrSA all have the same aromatic ring (benzene), while HNA and 7-BHNA are both naphthalene derivatives. The differences in the LSPR peak wavelengths obtained here should be mainly due to the functional groups on aromatic ring, and it appears that the introduction of the –Br and –COOH groups to the aromatic rings is beneficial for making GNRs with high ARs (long LSPR peak wavelengths).

The LSPR peak wavelengths of GNRs synthesized using 5-BrSA or 7-BrHNA are longer than those without using –Br. Thus, aromatic additives with a Br group may facilitate the preparation of high AR GNRs, possibly due to a relatively strong affinity of the Br atom with Au. Comparing the additives with the same functional group(s), GNRs synthesized with 5-BrSA has a longer LSPR peak wavelength than that with 7-BrHNA, and this is also true for SA and HNA. This indicates that the aromatic rings (benzene and naphthalene) in the additives also play certain roles in determining the AR of the GNRs, possibly due to the

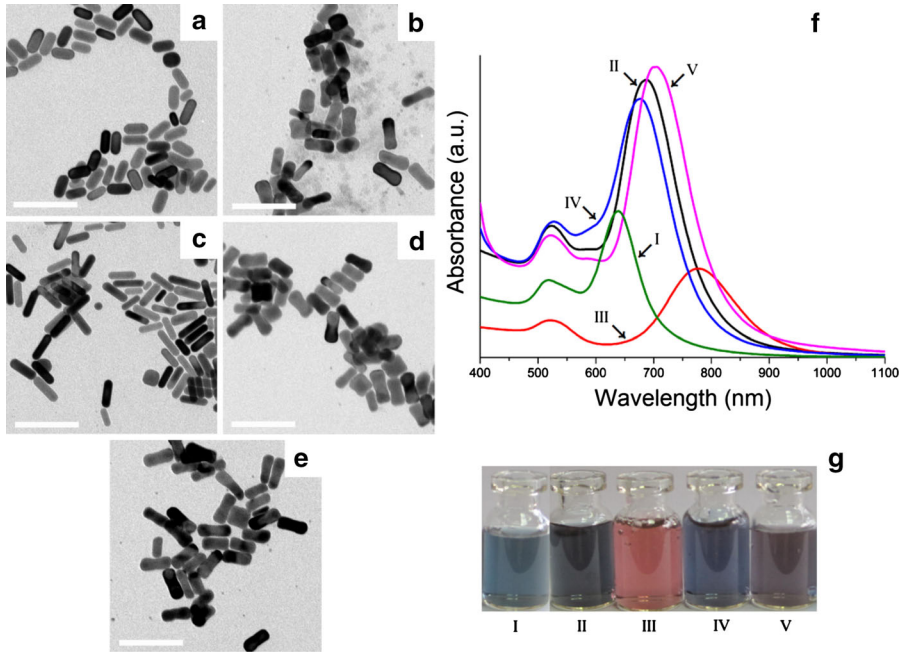

Fig. 2 Characterization of GNRs synthesized under the conditions specified in Table 1. TEM images of GNRs synthesized using PhOH (**a**), SA (**b**) 5-BrSA (**c**), HNA (**d**), or 7-BrHNA (**e**) as additive. UV–Vis–NIR spectra (**f**) of GNRs synthesized using PhOH (*I*), SA (*II*), 5-BrSA (*III*), HNA (*IV*), or 7-BrHNA (*V*) as additive, respectively. The photos (**g**) of GNR solutions synthesized using PhOH (*I*), SA (*II*), 5-BrSA (*III*), HNA (*IV*), or 7-BrHNA (*V*) as additive, respectively. *Scale bars*: 100 nm

Table 2 Comparison of the concentration, pH, dimensions, ARs, and LSPR peak wavelengths of the GNR solutions prepared in the presence of different aromatic additives[a]

Additive[b] (g)	C[c] (nM)	pH	Dimensions[d] (nm)	AR	LSPR peak wavelength (nm)
PhOH	0.57	3.00	(37.3 ± 2.2) × (17.4 ± 1.4)	~2.1	638
SA	0.89	2.53	(46.3 ± 4.6) × (19.3 ± 2.6)	~2.4	688
5-BrSA	0.22	2.51	(45.1 ± 3.4) × (13.6 ± 1.1)	~3.3	778
HNA	0.87	2.50	(43.4 ± 5.3) × (18.2 ± 3.0)	~2.4	676
7-BrHNA	0.88	2.51	(47.0 ± 4.8) × (18.9 ± 2.0)	~2.5	706

[a] The amounts of C16TABr, $AgNO_3$, AA, and seed solution used for GNR growth are 0.54 g, 480 μL, 300 μL, and 48 μL, respectively

[b] The concentration of additive in the growth solution used for GNR growth is 2.4 mM

[c] The calculated concentration of GNRs (Orendorff and Murphy 2006)

[d] Measured from Fig. 2a–e (At least 80 GNRs are counted for each set.)

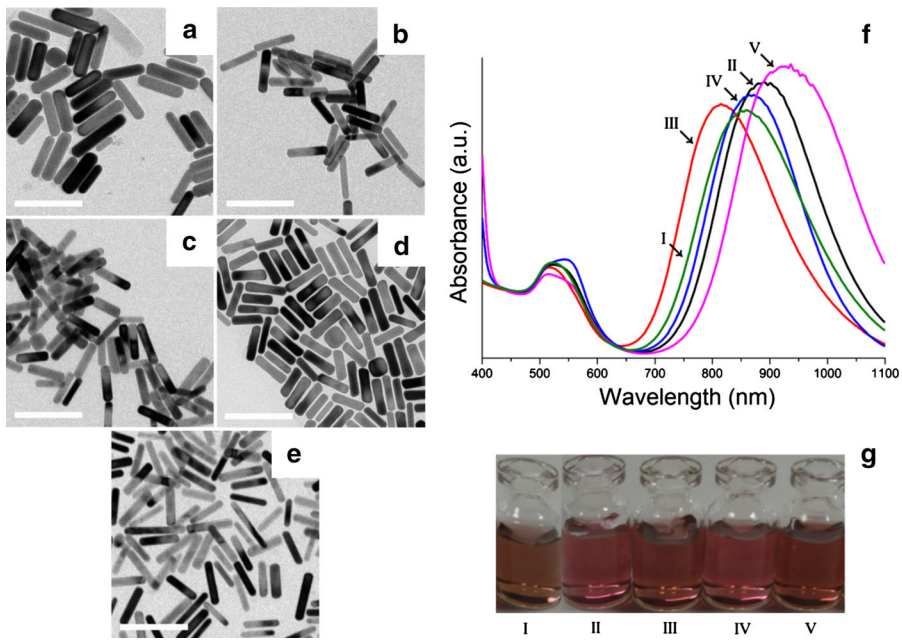

Fig. 3 Characterization of GNRs synthesized under the conditions specified in Table 3. TEM images of GNRs synthesized using PhOH (**a**), SA (**b**), 5-BrSA (**c**), HNA (**d**), or 7-BrHNA (**e**) as additive. UV–Vis–NIR spectra (**f**) of GNRs synthesized using PhOH (*I*), SA (*II*), 5-BrSA (*III*), HNA (*IV*), or 7-BrHNA (*V*) as additive, respectively. The photos (**g**) of GNR solutions synthesized using PhOH (*I*), SA (*II*), 5-BrSA (*III*), HNA (*IV*), or 7-BrHNA (*V*) as additive, respectively. *Scale bars*: 100 nm

different affinities of the aromatic rings to Au. Unlike the other four aromatic additives, PhOH does not contain a –COOH group and hence is a much weaker acid (pKa ~ 9) compared to others all containing a -COOH group (pKa ~ 4-5). As a result, the pH value of the resulting GNR solution with PhOH is higher (pH 3.00) than others (ca 2.5, see Table 2). The solution pH has been found to influence the AR (hence LSPR peak wavelength) of the synthesized GNRs (Wang et al. 2005; Ye et al. 2012; Zhu et al. 2010).

Effect of HCl

The effects of the aromatic additives on the GNR synthesis were changed dramatically when 300 μL (36 mmol) of concentrated HCl solution was added into the growth solution (Fig. 2, 3). The synthesized GNR solutions were light brown to light red, and the GNRs were mostly cylindrical shaped. The concentrations, dimensions, ARs, and LSPR peak wavelengths of the GNRs in the final solutions are listed in

Table 3 Concentrations, dimensions, ARs, and LSPR peak wavelengths of the GNR solutions prepared in the presence of aromatic additives with addition of 300 μL (36 mmol) concentrated HCl[a]

Additive[b] (g)	C[c] (nM)	Dimensions[d] (nm)	AR	LSPR peak wavelength (nm)
PhOH	0.59	(61.3 ± 6.0) × (16.1 ± 2.0)	~3.8	858
SA	0.61	(56.8 ± 5.6) × (13.3 ± 1.0)	~4.3	890
5-BrSA	0.67	(52.6 ± 4.8) × (14.3 ± 1.2)	~3.7	816
HNA	0.61	(51.8 ± 6.3) × (13.1 ± 1.5)	~4.0	872
7-BrHNA	0.61	(59.1 ± 6.0) × (12.9 ± 1.4)	~4.6	920

[a] The amounts of C16TABr, $AgNO_3$, AA, and seed solution used for GNR growth are 0.54 g, 480 μL, 300 μL, and 48 μL, respectively

[b] The concentration of additive in the growth solution used for GNR growth is 2.4 mM

[c] The calculated concentration of GNRs (Orendorff and Murphy 2006)

[d] Measured from Fig. 3a–e (At least 80 GNRs are counted for each set.)

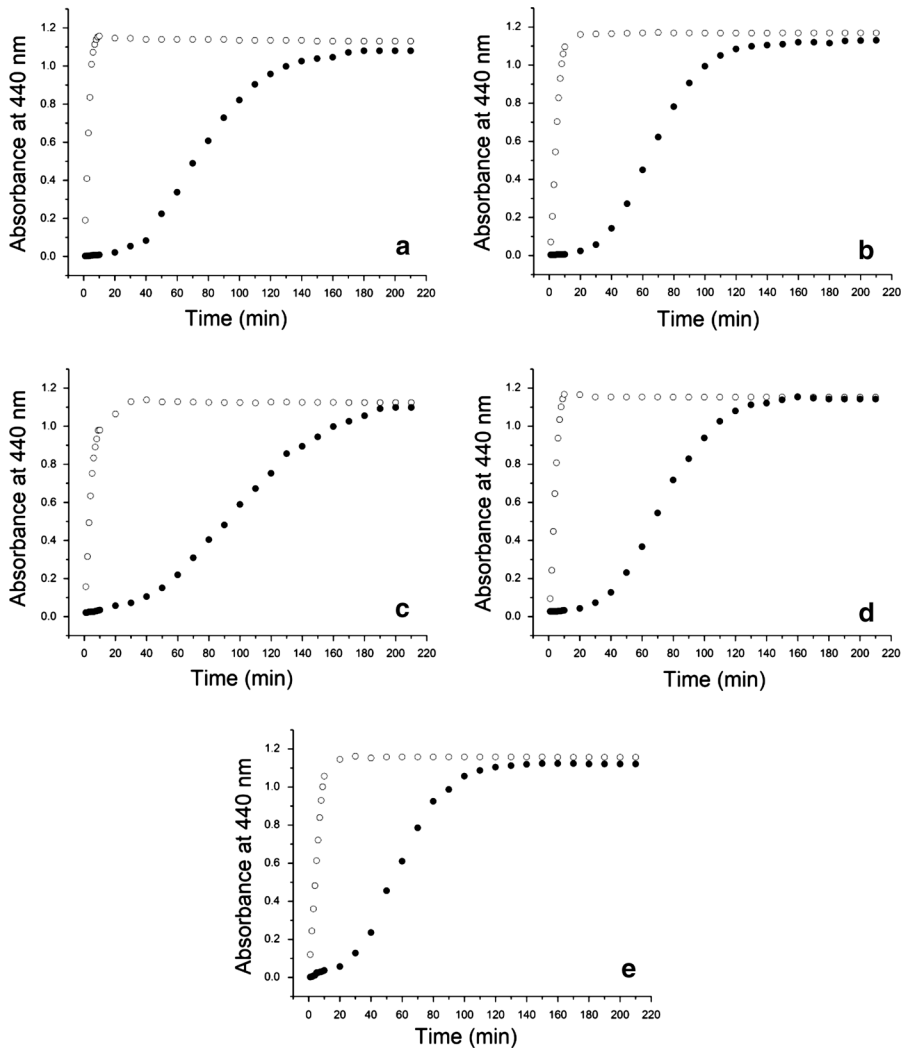

Fig. 4 Absorbances at 440 nm of the GNR growth solutions versus. time using different aromatic additives: PhOH (**a**), SA (**b**), 5-BrSA (**c**), HNA (**d**), or 7-BrHNA (**e**) with (lower pH, *solid circle*) and without (higher pH, *empty circle*) the addition of HCl

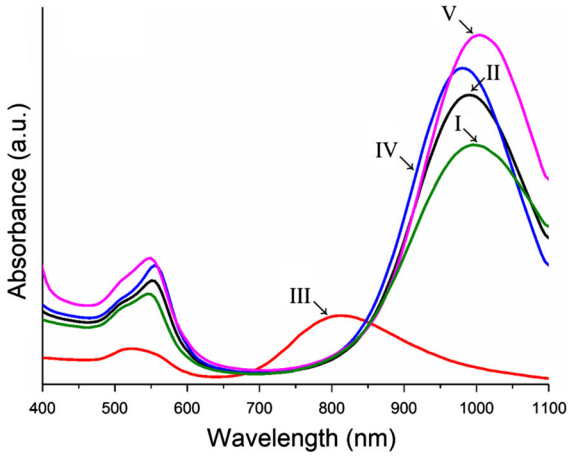

Fig. 5 UV–Vis–NIR spectra of the GNRs synthesized by using PhOH (*I*), SA (*II*), 5-BrSA (*III*), HNA (*IV*), or 7-BrHNA (*V*) as additives in the presence of HNO_3

Table 3. The AR of the GNRs was measured from the TEM images in Fig. 3a–e. The LSPR peak wavelength (λ_{LSPR}) of the GNRs is found to be positively and linearly correlated to the AR in Tables 2, 3 via Eq. (2.

$$\lambda_{LSPR} = 111.8 \times \text{AR} + 413.9. \quad (2)$$

The above equation clearly indicates that the LSPR peak wavelength is strongly dependent on the AR of GNRs (Lohse and Murphy 2013): the larger the AR, the longer the LSPR peak wavelength of GNRs. The TEM images of GNRs (Fig. 2a–e, 3a–e) are well correlated with their UV–Vis–NIR spectra (Fig. 2f, 3f).

Compared with Table 2, the concentrations of resulting GNRs are decreased from 0.87–0.89 to 0.61 nM for SA, HNA, and 7-BrHNA after the addition of HCl (Table 3). However, the GNR concentration with 5-BrSA is increased from 0.22 to 0.67 nM, while that for PhOH additive shows little difference. The LSPR peak wavelength order for the GNR solutions are as follows: 7-BrHNA (920 nm) > SA (890 nm) > HNA (872 nm) > PhOH (858 nm) > 5-BrSA (816 nm). This order is completely different from that obtained without the addition of HCl as mentioned above. Moreover, the LSPR bands are stronger and also appear at longer wavelengths. This indicates that the effect of HCl added on the synthesized GNRs is significant even in the presence of aromatic additives. This is unsurprising given the fact the formation of GNR (Eq. 1) does release HCl into the reaction media. In addition, many other factors could also influence the GNR growth, including formation of AgBr (Huang et al. 2009; Murphy et al. 2010), aromatic electron system on the GNR surfaces (Michota and Bukowska

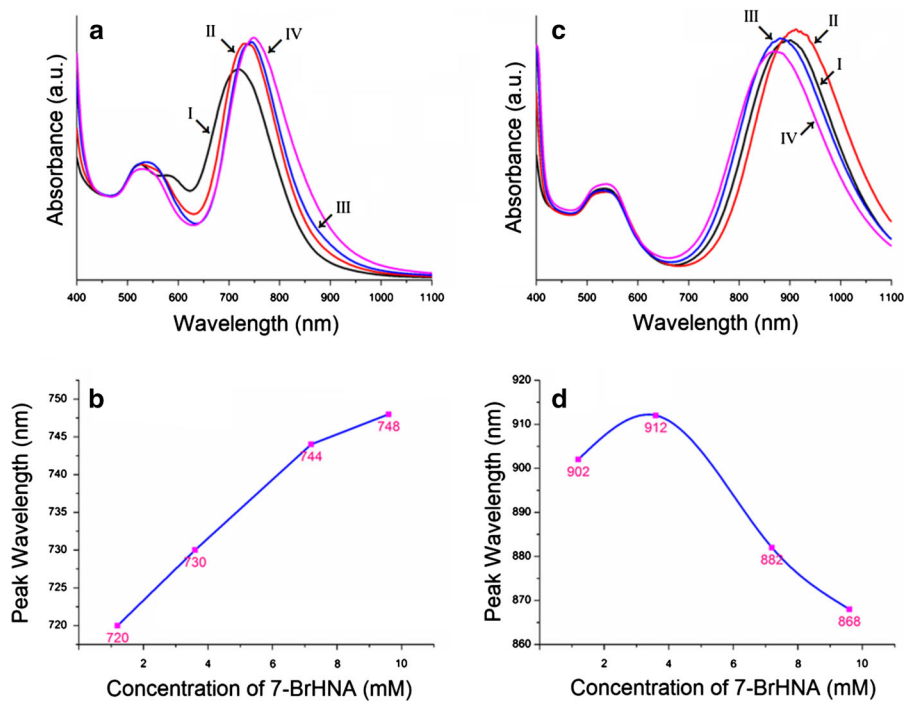

Fig. 6 Characterization of GNRs synthesized at different concentrations of 7-BrHNA as additive. UV–Vis–NIR spectra (**a**) and the LSPR peak wavelengths (**b**) of GNRs synthesized without the addition of HCl, UV–Vis–NIR spectra (**c**), and the LSPR peak wavelengths (**d**) of GNRs synthesized with the addition of 300 μL HCl. The concentrations of 7-BrHNA in the growth solution are 1.2 (*I*), 3.6 (*II*), 7.2 (*III*), 9.6 (*IV*) mM

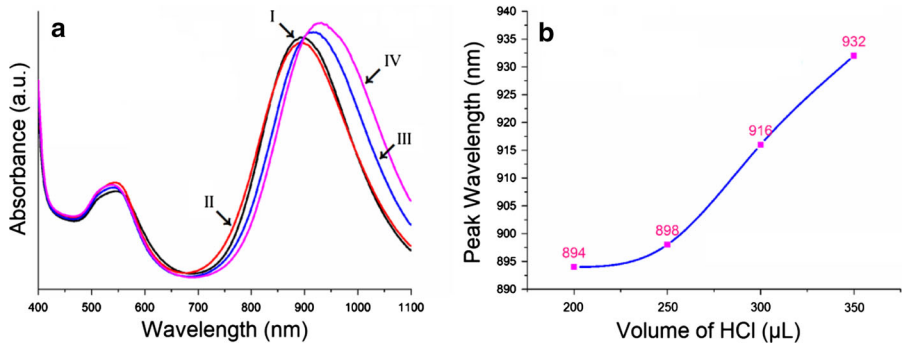

Fig. 7 Characterization of GNRs synthesized with 7-BrHNA as additive at different pH values. UV–Vis–NIR spectra (**a**) and LSPR peak wavelengths (**b**) of the synthesized GNRs. The volumes of HCl added are 200 (*I*), 250 (*II*), 300 (*III*), 350 (*IV*) μL

2003; Wang et al. 2010), and the reducing power of AA (Wang et al. 2005).

The reduction of gold ions into gold atoms can be determined by monitoring the optical absorbance of the GNR growth solutions at 440 nm (Rao and Doremus 1996, Sau and Murphy 2004). The stronger the absorbance, the more the gold atoms are formed. The change of the absorbance with time will reflect the reduction kinetics of gold precursor in the GNR growth solutions. After the addition of 36 mmol HCl into the growth solutions with different aromatic additives, the pH values of the resulting GNR growth solutions are reduced from 2.5 ~ 3.0 to 1.2, and the time to reach the absorbance plateau value (about 1.1) is prolonged from about 10 min to 2 ~ 3 h (Fig. 4). This indicates that the reduction of gold precursors is significantly slowed down. Wang et al. reported that the decreasing pH value of the GNR growth solution would lower the reducing power of AA and the reducing rate of gold ions (Wang et al. 2005).

The effects of the aromatic additives on the GNR synthesis were also changed dramatically when 36 mmol concentrated HNO_3 solution was added in the growth solution (Fig. 5). The LSPR peak wavelengths for the prepared GNR solutions are in the following order: 7-BrHNA (1005 nm) > PhOH (995 nm) > SA (990 nm) > HNA (980 nm) > 5-BrSA (815 nm). The LSPR peak wavelengths were obviously increased after the addition of HNO_3, similar to those observed with HCl. HNO_3 is a strong acid similar to HCl, but does not contain halides. The pH values of the resulting GNR solutions after the addition of 36 mmol HNO_3 are ~1.2, the same as those with HCl addition. The fact that the addition of HCl or HNO_3 yielded similar elongated GNR growth strongly suggests that pH plays an important role in determining the GNR growth. Given the fact that the LSPR peak appears at the longest wavelength (biggest AR) with 7-BrHNA after the addition of HCl or HNO_3, the effect of the 7-BrHNA concentration was further investigated.

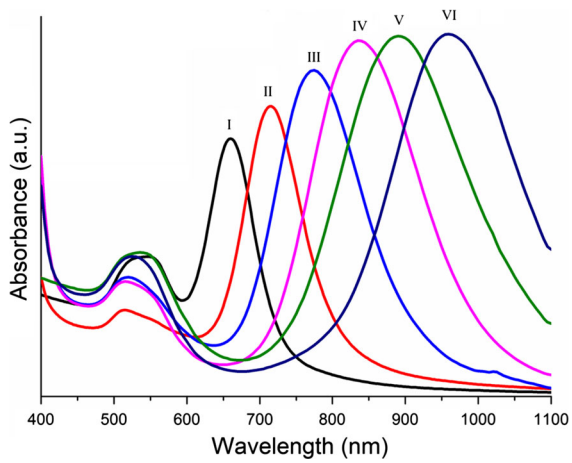

Fig. 8 UV–Vis–NIR spectra of the synthesized GNRs under the conditions in Table 4. The LSPR peaks of synthesized GNRs are 660 nm (*I*), 714 nm (*II*), 775 nm (*III*), 835 nm (*IV*), 890 nm (*V*), or 960 nm (*VI*), respectively

Effects of 7-BrHNA concentration

As shown in Fig. 6, the LSPR band of GNR solution increases from 720 to 748 nm as the concentration of 7-BrHNA is increased from 1.2 to 9.6 mM. Obviously, the concentration of the additive does have an

Table 4 Experimental conditions used for controlled synthesis of GNRs, ARs, and LSPR peak wavelengths of the GNR solutions[a]

7-BrHNA (g, mM)	$AgNO_3$ (mM)	HCl (mM)	AA (mM)	Seed solution (μL)	AR[b]	LSPR peak wavelength (nm)
0.08, 9.6	0.093	0	0.248	48	2.2	660
0.02, 2.4	0.031	0	0.248	48	2.7	714
0.08, 9.6	0.062	19.5	0.62	48	3.2	775
0.03, 3.6	0.062	19.5	0.31	48	3.8	835
0.04, 4.8	0.062	97.5	0.62	48	4.3	890
0.04, 4.8	0.093	97.5	0.62	96	4.9	960

[a] The amounts of C16TABr used for GNR growth is 0.54 g

[b] Estimated from Eq. (2)

impact on the GNR growth and the LSPR wavelength. Without the addition of HCl, there seems to be a trend that the more the additives present in the growth solution, the longer the LSPR peak wavelength for the obtained GNR. However, when HCl was added, there is a maximum LSPR peak wavelength of 912 nm for GNR prepared at 3.6 mM 7-BrHNA. Interestingly, at the same concentration as that of 7-BrHNA, the LSPR absorbance is stronger with the addition of HCl.

Effect of HCl amount

It remains a subject of considerable ongoing research interest how pH can be used to tune the LSPR wavelength of GNRs despite several reported researches (Busbee et al. 2003; Cheng et al. 2011; Ye et al. 2013, 2012; Zhu et al. 2010). Figure 7 shows that the LSPR peak wavelength is increased from 894 to 932 nm with the amount of HCl addition being increased from 200 to 350 μL. This indicates that the ARs of GNRs synthesized in the presence of 3.6 mM 7-BrHNA can also be adjusted by changing the amount of HCl added. The addition of HCl in the growth solution is beneficial for the preparation of GNRs with a larger AR and longer LSPR peak wavelength.

Controlled synthesis of GNRs

7-BrHNA is the most effective among the five aromatic additives studied here in terms of synthesizing GNRs with high ARs and long LSPR absorption bands. Figure 8 shows the absorption spectra of a range of GNRs synthesized with 7-BrHNA as additive, the LSPR bands of GNRs can be systematically adjusted from 660 to 960 nm by changing the amount of reactants (see Fig. 8 and Table 4).

Conclusion

In summary, monodisperse GNRs are successfully synthesized via a seeded growth approach in the presence of five different aromatic additives (PhOH, SA, 5-BrSA, HNA, or 7-BrHNA). The LSPR wavelength of the synthesized GNRs can be systematically adjusted in the NIR region, providing a facile, controllable way for preparation of GNRs with the preferred optical properties that may have broad biomedical applications. 7-BrHNA, a –Br, and –COOH containing aromatic additive, is the most effective among the five aromatic additives studied here in terms of synthesizing GNRs with high ARs and long LSPR absorption bands.

Acknowledgments This work is supported by National Natural Science Foundation of China (NSFC, Grant No.81171439), the National Key Technology R&D Program of the Ministry of Science and Technology (2012BAI18B01), the European Union Marie Curie Action via a Marie Curie International Incoming Fellowship to S.G. (Grant No. PIIF-GA-2012-331281), and the University of Leeds (UK).

References

Almora-Barrios N, Novell-Leruth G, Whiting P, Liz-Marzán LM, López N (2014) Theoretical description of the role of halides, silver, and surfactants on the structure of gold nanorods. Nano Lett 14:871–875. doi:10.1021/nl404661u

Busbee BD, Obare SO, Murphy CJ (2003) An improved synthesis of high-aspect-ratio gold nanorods. Adv Mater 15:414–416. doi:10.1002/adma.200390095

Charan S, Sanjiv K, Singh N, Chien F-C, Chen Y-F, Nergui NN, Huang S-H, Kuo CW, Lee T-C, Chen P (2012) Development of chitosan oligosaccharide-modified gold nanorods for in vivo targeted delivery and noninvasive imaging by NIR irradiation. Bioconjug Chem 23:2173–2182. doi:10.1021/bc3001276

Cheng J, Ge L, Xiong B, He Y (2011) Investigation of pH effect on gold nanorod synthesis. J Chin Chem Soc 58:822–827. doi:10.1002/jccs.201190128

Edgar JA, McDonagh AM, Cortie MB (2012) Formation of gold nanorods by a stochastic "popcorn" mechanism. ACS Nano 6:1116–1125. doi:10.1021/nn203586j

Gai PL, Harmer MA (2002) Surface atomic defect structures and growth of gold nanorods. Nano Lett 2:771–774. doi:10.1021/nl0202556

Garg N, Scholl C, Mohanty A, Jin R (2010) The role of bromide ions in seeding growth of Au nanorods. Langmuir 26:10271–10276. doi:10.1021/la100446q

Gomez-Grana S, Hubert F, Testard F, Guerrero-Martínez A, Grillo I, Liz-Marzán LM, Spalla O (2011) Surfactant (bi) layers on gold nanorods. Langmuir 28:1453–1459. doi:10.1021/la203451p

Grzelczak M, Pérez-Juste J, Mulvaney P, Liz-Marzán LM (2008) Shape control in gold nanoparticle synthesis. Chem Soc Rev 37:1783–1791. doi:10.1039/B711490G

Hassan P, Yakhmi J (2000) Growth of cationic micelles in the presence of organic additives. Langmuir 16:7187–7191. doi:10.1021/la000517o

Huang X, Neretina S, El-Sayed MA (2009) Gold nanorods: from synthesis and properties to biological and biomedical applications. Adv Mater 21:4880–4910. doi:10.1002/adma.200802789

Huang H, Li C, Qu C, Huang S, Liu F, Zeng Y (2012) Sensitive detection of DNA based on the optical properties of core–shell gold nanorods. J Nanopart Res 14:1–7. doi:10.1007/s11051-012-0754-3

Jana NR, Gearheart L, Murphy CJ (2001) Wet chemical synthesis of high aspect ratio cylindrical gold nanorods. J Phys Chem B 105:4065–4067. doi:10.1021/jp0107964

Johnson CJ, Dujardin E, Davis SA, Murphy CJ, Mann S (2002) Growth and form of gold nanorods prepared by seed-mediated, surfactant-directed synthesis. J Mater Chem 12:1765–1770. doi:10.1039/B200953F

Lai J, Zhang L, Niu W, Qi W, Zhao J, Liu Z, Zhang W, Xu G (2014) One-pot synthesis of gold nanorods using binary surfactant systems with improved monodispersity, dimensional tunability and plasmon resonance scattering properties. Nanotechnology 25:125601. doi:10.1088/0957-4484/25/12/125601

Lin Z, Cai J, Scriven L, Davis H (1994) Spherical-to-wormlike micelle transition in CTAB solutions. J Phys Chem 98:5984–5993. doi:10.1021/j100074a027

Liu X, Huang N, Li H, Wang H, Jin Q, Ji J (2014) Multidentate polyethylene glycol modified gold nanorods for in vivo near-infrared photothermal cancer therapy. ACS Appl Mater Interfaces 6:5657–5668. doi:10.1021/am5001823

Lohse SE, Murphy CJ (2013) The quest for shape control: a history of gold nanorod synthesis. Chem Mater 25:1250–1261. doi:10.1021/cm303708p

Menon D, Basanth A, Retnakumari A, Manzoor K, Nair SV (2012) Green synthesis of biocompatible gold nanocrystals with tunable surface plasmon resonance using garlic phytochemicals. J Biomed Nanotechnol 8:901–911. doi:10.1166/jbn.2012.1455

Michota A, Bukowska J (2003) Surface-enhanced Raman scattering (SERS) of 4-mercaptobenzoic acid on silver and gold substrates. J Raman Spectrosc 34:21–25. doi:10.1002/jrs.928

Murphy CJ, Sau TK, Gole AM, Orendorff CJ, Gao J, Gou L, Hunyadi SE, Li T (2005) Anisotropic metal nanoparticles: synthesis, assembly, and optical applications. J Phys Chem B 109:13857–13870. doi:10.1021/jp0516846

Murphy CJ, Thompson LB, Alkilany AM, Sisco PN, Boulos SP, Sivapalan ST, Yang JA, Chernak DJ, Huang J (2010) The many faces of gold nanorods. J Phys Chem Lett 1:2867–2875. doi:10.1021/jz100992x

Nikoobakht B, El-Sayed MA (2003) Preparation and growth mechanism of gold nanorods (NRs) using seed-mediated growth method. Chem Mater 15:1957–1962. doi:10.1021/cm020732l

Orendorff CJ, Murphy CJ (2006) Quantitation of metal content in the silver-assisted growth of gold nanorods. J Phys Chem B 110:3990–3994. doi:10.1021/jp0570972

Rao P, Doremus R (1996) Kinetics of growth of nanosized gold clusters in glass. J Non Cryst Solids 203:202–205. doi:10.1016/0022-3093(96)00483-8

Sau TK, Murphy CJ (2004) Seeded high yield synthesis of short Au nanorods in aqueous solution. Langmuir 20:6414–6420. doi:10.1021/la049463z

Sharma V, Park K, Srinivasarao M (2009) Colloidal dispersion of gold nanorods: historical background, optical properties, seed-mediated synthesis, shape separation and self-assembly. Mater Sci Eng R Rep 65:1–38. doi:10.1016/j.mser.2009.02.002

Si S, Leduc C, Delville MH, Lounis B (2012) Short gold nanorod growth revisited: the critical role of the bromide counterion. ChemPhysChem 13:193–202. doi:10.1002/cphc.201100710

Song J, Pu L, Zhou J, Duan B, Duan H (2013) Biodegradable theranostic plasmonic vesicles of amphiphilic gold nanorods. ACS Nano 7:9947–9960. doi:10.1021/nn403846v

Tian Y, Chen L, Zhang J, Ma Z, Song C (2012) Bifunctional Au-nanorod@ Fe3O4 nanocomposites: synthesis, characterization, and their use as bioprobes. J Nanopart Res 14:1–11. doi:10.1007/s11051-012-0998-y

Wadams RC, Fabris L, Vaia RA, Park K (2013) Time-dependent susceptibility of the growth of gold nanorods to the addition of a cosurfactant. Chem Mater 25:4772–4780. doi:10.1021/cm402863h

Wang C, Wang T, Ma Z, Su Z (2005) pH-tuned synthesis of gold nanostructures from gold nanorods with different aspect ratios. Nanotechnology 16:2555. doi:10.1088/0957-4484/16/11/015

Wang Z, Zong S, Yang J, Song C, Li J, Cui Y (2010) One-step functionalized gold nanorods as intracellular probe with improved SERS performance and reduced cytotoxicity.

Biosens Bioelectron 26:241–247. doi:10.1016/j.bios.2010.06.032

Wang C-H, Chang C-W, Peng C-A (2011) Gold nanorod stabilized by thiolated chitosan as photothermal absorber for cancer cell treatment. J Nanopart Res 13:2749–2758. doi:10.1007/s11051-010-0162-5

Wang X, Shao M, Zhang S, Liu X (2013) Biomedical applications of gold nanorod-based multifunctional nano-carriers. J Nanopart Res 15:1–16. doi:10.1007/s11051-013-1892-y

Xu C, Yang D, Mei L, Lu B, Chen L, Li Q, Zhu H, Wang T (2013) Encapsulating gold nanoparticles or nanorods in graphene oxide shells as a novel gene vector. ACS Appl Mater Interfaces 5:2715–2724. doi:10.1021/am400212j

Ye X, Jin L, Caglayan H, Chen J, Xing G, Zheng C, Doan-Nguyen V, Kang Y, Engheta N, Kagan CR, Murray CB (2012) Improved size-tunable synthesis of monodisperse gold nanorods through the use of aromatic additives. ACS Nano 6:2804–2817. doi:10.1021/nn300315j

Ye X, Gao Y, Chen J, Reifsnyder DC, Zheng C, Murray CB (2013) Seeded growth of monodisperse gold nanorods using bromide-free surfactant mixtures. Nano Lett 13:2163–2171. doi:10.1021/nl400653s

Yoo H, Sharma J, Yeh H-C, Martinez JS (2010) Solution-phase synthesis of Au fibers using rod-shaped micelles as shape directing agents. Chem Commun 46:6813–6815. doi:10.1039/C0CC02100H

Zhong Y, Wang C, Cheng L, Meng F, Zhong Z, Liu Z (2013) Gold nanorod-cored biodegradable micelles as a robust and remotely controllable doxorubicin release system for potent inhibition of drug-sensitive and-resistant cancer cells. Biomacromolecules 14:2411–2419. doi:10.1021/bm400530d

Zhu J, Yong KT, Roy I, Hu R, Ding H, Zhao L, Swihart MT, He GS, Cui Y, Prasad PN (2010) Additive controlled synthesis of gold nanorods (GNRs) for two-photon luminescence imaging of cancer cells. Nanotechnology 21:285106. doi:10.1088/0957-4484/21/28/285106